

# Model Equation for Predicting the Tensile Strength of Resistance-Brazed Joints

*The tensile strength of resistance-brazed joints is predicted using a model equation based on the electric current variation*

BY K. TAKESHITA

**ABSTRACT.** To ensure the quality of a resistance-brazed joint, a model equation for predicting its tensile strength is presented on the basis of the electric current variation during resistance brazing. The model equation derived considers changes occurring in a joint during resistance brazing and is subsequently expressed in a polynomial in three variables of  $i_1$ ,  $i_1-i_2$ , and  $i_2/i_3$ ;  $i_1$  is the first maximum value,  $i_2$  the minimum value and  $i_3$  the second maximum value in the electric current measurement. The predicted tensile strength is discussed and compared with experimental data obtained from Ti-10 wt-% Zr alloy joints resistance brazed with Ti-20 wt-% Zr-20 wt-% Ni-20 wt-% Cu or Ni-50 wt-% Cu filler metal.

## Introduction

In resistance brazing, the heat is obtained from dynamic resistance to the flow of electric current passing through a joint. The process is rapid, and the heating zones can be confined to very small areas. These characteristics provide the following advantages from a production viewpoint: 1) a high level of productivity, 2) suitability for automation and 3) decreased base-metal degradation. However, the dynamic resistance of each run can vary, which causes inconsistency in the joint. Thus, to ensure the quality of a resistance-brazed joint, its strength must be predicted without mechanical tests. Since the electric current during resistance brazing is inversely proportional to the dynamic resistance, it provides useful information on the changes that occur in a joint during resistance brazing.

The present paper proposes a model equation for predicting the tensile strength of a resistance-brazed joint on

the basis of the electric current variation during resistance brazing. The efficacy of the model equation is subsequently determined in comparison with experimental data.

## Experimental Procedures

Ti-10 wt-% Zr alloy rods 4 mm (0.157 in.) in diameter were butt-joint resistance brazed with Ti-20 wt-% Zr-20 wt-% Ni-20 wt-% Cu or Ni-50 wt-% Cu filler metal foils of 50  $\mu\text{m}$  (0.00197 in.) thickness under a protective argon gas atmosphere, as shown in Fig. 1A. The energizing AC voltage was set at 5.7 V, the energizing time at 0.8 s and the applied pressure at 0.63 MPa (0.0914 ksi). The Ti-10 wt-% Zr alloy rod was used as a base metal as cold drawn by a reduction in cross-sectional area of 60%; its tensile strength was 900 MPa (131 ksi). The physical properties of the materials used for resistance brazing are listed in Table 1. The surfaces of the base metal to be resistance brazed had an arithmetic average surface roughness of 0.4  $\mu\text{m}$  (0.0000157 in). Before resistance brazing, the base metal and the filler metal foils were degreased in an ultrasonically agitated bath of acetone and then rinsed in distilled water. The resistance-brazed joint was ma-

chined to form the tensile test specimen, the shape and size of which are shown in Fig. 1B. Tension tests were conducted at room temperature using an Instron-type test machine at a cross-head speed of 0.05 mm/s (0.00197 in./s).

During each resistance brazing, the electric current passing through the primary circuit of a transformer with an input voltage of 200 V of AC was recorded using an AC current/DC voltage transducer, with a response time of 0.25 s, and a storage oscilloscope, as shown in Fig. 2.

## Experimental Results

### Tensile Strength of the Joints

Figure 3 shows the histogram for the measured tensile strength of 46 joints resistance brazed with Ti-Zr-Ni-Cu filler metal by a class interval of 30 MPa (4.35 ksi). The tensile strength varied from 260 to 485 MPa (37.7 to 70.3 ksi). The arithmetic mean value was 397 MPa (57.6 ksi), and the standard deviation was 39.7 MPa (5.76 ksi). Figure 4 shows the histogram for the measured tensile strength of 46 joints resistance brazed with Ni-Cu filler metal by a class interval of 40 MPa (5.80 ksi). The tensile strength varied from 138 to 508 MPa (20.0 to 73.7 ksi). The arithmetic mean value was 281 MPa (40.8 ksi), and the standard deviation was 83.6 MPa (12.1 ksi). These results demonstrate that, regardless of the filler metal, the tensile strength of the resistance-brazed joints varies over a wide range, even though the same brazing procedure was employed each time.

### Electric Current during Resistance Brazing

Figure 5 shows a typical electric current curve recorded during resistance brazing with Ti-Zr-Ni-Cu filler metal in which the following four stages can be identified:

## KEY WORDS

Resistance Brazing  
Butt Joint  
Quality Assurance  
Tensile Strength  
Electrical Data  
Titanium Alloy  
Titanium Brazing Filler Metal

K. TAKESHITA is with the Dept. of Mechanical Engineering, Fukui University, Fukui, Japan.



Since the contact area between the filler metal and base metals is presumably proportional to the first maximum value in the electric current curve,  $i_1$ , the requirement for the optimal contact area leads to that for the optimal value of  $i_1$ . The increase in temperature of the joint, as mentioned earlier, is associated with the difference between the first maximum value and the minimum value in the electric current curve,  $i_1-i_2$ . If, for simplicity, the increase in temperature of the joint is assumed to be linearly related to the value of  $i_1-i_2$ , the requirement for the optimal temperature of the joint leads to that for the optimal value of  $i_1-i_2$ . Thus, the first part of Assumption 1 is modified to the following assumption (labeled A1-1) using the first maximum value,  $i_1$ , and the minimum value,  $i_2$ , in the electric current curve.

**A1-1:** The joint demonstrates its maximum tensile strength when the values of  $i_1$  and  $i_1-i_2$  are both optimal.

The latter part of Assumption 1 can also be modified to allow derivation of the model equation and incorporate Assumption 3, discussed below. If it is assumed the spacing between the base metals varies from  $S_2$  to  $S_3$  in stage 3 and the resistance of the base metals,  $R_b$ , and the electrical resistivity of the filler metal,  $\rho_f$ , remain unchanged during stage 3,  $S_2$  and  $S_3$  are given by

$$S_2 = \frac{V_e - R_b \cdot i_2}{\rho_f \cdot i_2} \quad (1)$$

$$S_3 = \frac{V_e - R_b \cdot i_3}{\rho_f \cdot i_3} \quad (2)$$

where  $V_e$  is the voltage applied to the joint,  $i_2$  is the electric current passing through the joint at the beginning of stage 3, identical to the minimum value in the electric current curve, and  $i_3$  is the electric current passing through the joint at the end of stage 3, identical to the second maximum value in the electric current curve.

Elimination of  $V_e$  from Equations 1 and 2 gives the following equation:

$$S_3 = \left( S_2 + \frac{R_b}{\rho_f} \right) \cdot \left( \frac{i_2}{i_3} \right) - \frac{R_b}{\rho_f} \quad (3)$$

Because  $S_2$  is approximately equal to the thickness of the filler metal, it can be regarded as a constant. If the value of  $R_b/\rho_f$  is assumed to be unchanged regardless of the joint temperature during stage 3 in each run, Equation 3 expresses Assumption 3 described above. The combination of the latter part of Assumptions 1 and 3 gives the following assumption:

**A1-2:** The joint demonstrates its maximum tensile strength when the value of  $i_2/i_3$  is optimal.

A1-1 and A1-2 allow the model equation for predicting the tensile strength of the joint to be expressed in a dimensionless form, as

$$\hat{\sigma} = \left( 1 + \beta x_1 + \alpha x_1^2 \right) \cdot \left( 1 + \delta x_2 + \gamma x_2^2 \right) \cdot \left( 1 + \xi x_3 + \eta x_3^2 \right) \quad (4)$$

where  $\hat{\sigma}$  is the predicted dimensionless tensile strength defined by  $\hat{\sigma}/\sigma_B^*$ ,  $x_1$ ,  $x_2$ , and  $x_3$  are dimensionless, independent variables defined by  $x_1 = (i_1/i_1^*) - 1$ ,  $x_2 = (i_1 - i_2)/(i_1^* - i_2^*) - 1$  and  $x_3 = (i_2/i_3)/(i_2^*/i_3^*) - 1$ ; and  $\alpha$ ,  $\beta$ ,  $\gamma$ ,  $\delta$ ,  $\xi$  and  $\eta$  are unknown parameters.  $\sigma_B^*$  is the predicted tensile strength of the joint resistance brazed with the electric current curve having the three extremum values of  $i_1$ ,  $i_2$  and  $i_3$ . Symbols denoted with an asterisk,  $\sigma_B^*$ ,  $i_1^*$ ,  $i_2^*$  and  $i_3^*$ , are the reference standard quantities introduced for the dimensionless expression to the model equation. In the present work,  $\sigma_B^*$  was set at the highest measured tensile strength among the joints. In addition,  $i_1^*$ ,  $i_2^*$  and  $i_3^*$  were set at the measured three extremum values in the electric current curve corresponding to the joint with the highest measured tensile strength,  $\sigma_B^*$ .

#### Modification of Model Equation

The values of the unknown parameters in Equation 4 may be determined by the least-squares method when experimental data are available. However, the calculation is too difficult to carry out because Equation 4 is nonlinear with respect to the unknown parameters. Thus, Equation 4 is modified to the linear form with respect to  $C_i$ , as

$$\hat{\sigma} = \sum_{i=0}^{26} C_i y_i \quad (5)$$

where  $C_0$  through  $C_{26}$  are unknown parameters, and  $y_0$  through  $y_{26}$  are defined by

$$\begin{aligned} y_0 &= 1, \quad y_1 = x_1, \quad y_2 = x_2, \quad y_3 = x_3, \quad y_4 = x_1^2, \quad y_5 = x_2^2, \quad y_6 = x_3^2, \\ y_7 &= x_1 x_2, \quad y_8 = x_2 x_3, \quad y_9 = x_3 x_1, \quad y_{10} = x_1^2 x_2, \quad y_{11} = x_1 x_2^2, \quad y_{12} = x_2^2 x_3, \quad y_{13} = x_2 x_3^2, \\ y_{14} &= x_3^2 x_1, \quad y_{15} = x_3 x_1^2, \quad y_{16} = x_1 x_2 x_3, \quad y_{17} = x_1^2 x_2^2, \quad y_{18} = x_2^2 x_3^2, \quad y_{19} = x_3^2 x_1^2, \\ y_{20} &= x_1^2 x_2 x_3, \quad y_{21} = x_1 x_2^2 x_3, \quad y_{22} = x_1 x_2 x_3^2, \quad y_{23} = x_1 x_2^2 x_3^2, \\ y_{24} &= x_1^2 x_2 x_3^2, \quad y_{25} = x_1^2 x_2^2 x_3, \quad y_{26} = x_1^2 x_2^2 x_3^2. \end{aligned} \quad (6)$$

Equation 5 can be derived by expanding Equation 4 and taking each term as an independent one. From the definitions of  $y_i$ , note that Equation 5 is a polynomial in the three variables of  $x_1$ ,  $x_2$  and  $x_3$ . To determine the values of  $C_i$  in Equation 5 by the least-squares method using experimental data, all the variables  $y_i$  must be independent of each other (Ref. 8). However, there is a strong correlation between  $y_1$  and  $y_4$ ,  $y_2$  and  $y_5$ ,  $y_3$  and  $y_6$ ,  $y_7$  and  $y_{17}$ ,  $y_8$  and  $y_{18}$ ,  $y_9$  and  $y_{19}$  and  $y_{16}$  and  $y_{26}$ , as  $y_4 = y_1^2$ ,  $y_5 = y_2^2$ ,  $y_6 = y_3^2$ ,  $y_{17} = y_7^2$ ,  $y_{18} = y_8^2$ ,  $y_{19} = y_9^2$  and  $y_{26} = y_{16}^2$ . These strong correlations may be considerably weakened by converting the variables  $y_i$  into the variables  $z_i$ , defined by the following (Ref. 9):

$$\begin{aligned} z_0 &= 1, \quad z_1 = x_1, \quad z_2 = x_2, \quad z_3 = x_3, \quad z_4 = (x_1 - \bar{x}_1)^2, \\ z_5 &= (x_2 - \bar{x}_2)^2, \quad z_6 = (x_3 - \bar{x}_3)^2, \quad z_7 = (x_1 - \bar{x}_1) \cdot (x_2 - \bar{x}_2), \\ z_8 &= (x_2 - \bar{x}_2) \cdot (x_3 - \bar{x}_3), \quad z_9 = (x_3 - \bar{x}_3) \cdot (x_1 - \bar{x}_1), \\ z_{10} &= (x_1 - \bar{x}_1)^2 \cdot (x_2 - \bar{x}_2), \quad z_{11} = (x_1 - \bar{x}_1) \cdot (x_2 - \bar{x}_2)^2, \\ z_{12} &= (x_2 - \bar{x}_2)^2 \cdot (x_3 - \bar{x}_3), \quad z_{13} = (x_2 - \bar{x}_2) \cdot (x_3 - \bar{x}_3)^2, \\ z_{14} &= (x_3 - \bar{x}_3)^2 \cdot (x_1 - \bar{x}_1), \quad z_{15} = (x_3 - \bar{x}_3) \cdot (x_1 - \bar{x}_1)^2, \\ z_{16} &= (x_1 - \bar{x}_1) \cdot (x_2 - \bar{x}_2) \cdot (x_3 - \bar{x}_3), \quad z_{17} = (x_1 - \bar{x}_1)^2 \cdot (x_2 - \bar{x}_2)^2, \\ z_{18} &= (x_2 - \bar{x}_2)^2 \cdot (x_3 - \bar{x}_3)^2, \quad z_{19} = (x_3 - \bar{x}_3)^2 \cdot (x_1 - \bar{x}_1)^2, \\ z_{20} &= (x_1 - \bar{x}_1)^2 \cdot (x_2 - \bar{x}_2) \cdot (x_3 - \bar{x}_3), \quad z_{21} = (x_1 - \bar{x}_1) \cdot (x_2 - \bar{x}_2)^2 \cdot (x_3 - \bar{x}_3), \\ z_{22} &= (x_1 - \bar{x}_1) \cdot (x_2 - \bar{x}_2) \cdot (x_3 - \bar{x}_3)^2, \quad z_{23} = (x_1 - \bar{x}_1) \cdot (x_2 - \bar{x}_2)^2 \cdot (x_3 - \bar{x}_3)^2, \\ z_{24} &= (x_1 - \bar{x}_1)^2 \cdot (x_2 - \bar{x}_2) \cdot (x_3 - \bar{x}_3)^2, \quad z_{25} = (x_1 - \bar{x}_1)^2 \cdot (x_2 - \bar{x}_2)^2 \cdot (x_3 - \bar{x}_3), \\ \text{and } z_{26} &= (x_1 - \bar{x}_1)^2 \cdot (x_2 - \bar{x}_2)^2 \cdot (x_3 - \bar{x}_3)^2 \end{aligned}$$

where  $\bar{x}_1$ ,  $\bar{x}_2$  and  $\bar{x}_3$  are the arithmetic means of  $x_1$ ,  $x_2$  and  $x_3$ , respectively.

Equation 5 is further rewritten with the variables  $z_i$  as the following:

$$\hat{\sigma} = \sum_{i=0}^{26} C'_i z_i \quad (7)$$

where  $C'_0$  through  $C'_{26}$  are unknown parameters, the values of which can be determined by the least-squares method using experimental data.

The coefficient of each similar term in Equation 5 should be equal to that of the corresponding similar term in the expansion equation of Equation 7. This requirement provides 26 equations connecting  $C_i$  in Equation 5 and  $C'_i$  in Equation 7. Thus, the values of  $C_i$  in Equation 5 are straightforwardly obtained using the 26 equations and the determined values of  $C'_i$  in Equation 7.

#### Calculated Results

The determined model expressed in Equation 5 is given by

$$\begin{aligned} \hat{\sigma} &= 0.990267 - 5.40196y_1 + 0.349258y_2 - 20.5886y_3 - 128.124y_4 + 0.631925y_5 + 786.873y_6 + 3.70242y_7 - 47.0691y_8 + 568.712y_9 + 238.990y_{10} + 16.7892y_{11} - 93.2564y_{12} + 2371.87y_{13} - 18882.5y_{14} + 20536.1y_{15} + 880.058y_{16} - 249.690y_{17} + 862.649y_{18} - 857794y_{19} - 43648.6y_{20} - \end{aligned}$$

$$1376.69y_{21} - 67812.3y_{22} + 52679.7y_{23} + 1863560y_{24} + 29622.9y_{25} - 1002250y_{26} \quad (8)$$

for the joints resistance brazed with Ti-Zr-Ni-Cu filler metal and

$$\begin{aligned} \hat{\sigma} = & 0.471453 - 0.0706636y_1 + 0.0708294y_2 + 2.05003y_3 + 0.330522y_4 \\ & + 0.0459062y_5 - 31.3718y_6 - 0.776454y_7 + 7.90254y_8 + 10.0663y_9 + \\ & 1.32587y_{10} - 0.997871y_{11} - 2.57078y_{12} - \\ & 17.0537y_{13} - 397.840y_{14} - 33.8689y_{15} + \\ & 29.8881y_{16} + 0.805031y_{17} - 64.3148y_{18} \\ & + 1.94237y_{19} - 10.6362y_{20} - \\ & 0.190932y_{21} + 191.315y_{22} + 227.238y_{23} \\ & + 167.302y_{24} - 6.27958y_{25} - 237.479y_{26} \quad (9) \end{aligned}$$

for the joints resistance brazed with Ni-Cu filler metal. The values of the reference standard quantities,  $\sigma_B^*$ ,  $i_1^*$ ,  $i_2^*$  and  $i_3^*$ , are 485 MPa (70.3 ksi), 33.3 A, 31.3 A and 32.2 A for Equation 8 and 508 MPa (73.7 ksi), 40.4 A, 34.1 A and 34.8 A for Equation 9, respectively. As mentioned previously, each set of values corresponds to the joint with the highest measured tensile strength among the joints. When the three extremum values in the electric current curve measured —  $i_1$ ,  $i_2$  and  $i_3$  — are given, the values of the dimensionless variables of  $y_1$  through  $y_{26}$  in Equations 8 and 9 can be determined using Equation 6 and the definitions of  $x_1$ ,  $x_2$  and  $x_3$ . Thus, Equations 8 and 9 enable prediction of the dimensionless tensile strength of the resistance-brazed joints. The predicted dimensionless tensile strength,  $\hat{\sigma}$ , can be transformed to the dimensional tensile strength,  $\hat{\sigma}_B$ , using the definition  $\hat{\sigma}_B = \hat{\sigma} \cdot \sigma_B^*$ .

Figure 6 shows the relationship between the tensile strength predicted by Equation 8 and the measured tensile strength for the joints resistance brazed with Ti-Zr-Ni-Cu filler metal. Figure 7 also shows the relationship between the tensile strength predicted by Equation 9 and the measured tensile strength for the joints resistance brazed with Ni-Cu filler metal. If the predictions are perfect, all data points plotted in Figs. 6 and 7 should lie on the solid straight lines drawn in these figures. However, these figures indicate there is some degree of variability. From the evaluation of the multiple correlation coefficient adjusted for the degrees of freedom, the efficacy of Equations 8 and 9 as a predictor can be assessed (Ref. 10). The closer the value is to unity, the greater the fitting quality and prediction accuracy of the equation. The calculations show the values are 0.883 for Equation 8 and 0.884 for Equation 9, indicating they are relatively close to unity. The root-mean-square error

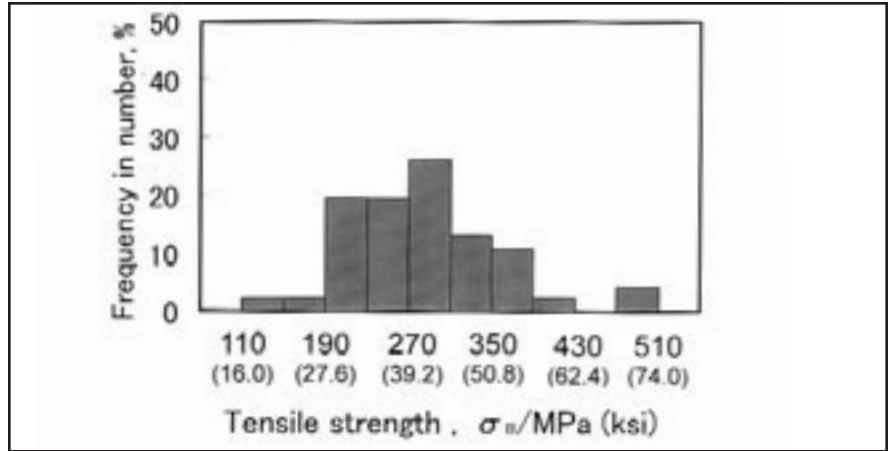


Fig. 4 — Histogram for measured tensile strength of joints resistance brazed with Ni-Cu filler metal.

(RMSE) of prediction gives an estimate of standard deviation of prediction residual that can be used to evaluate the approximate confidence interval, explained below.

A 95% confidence interval =  $\pm 1.96$  RMSE (Ref.11). The 95% confidence interval is  $\pm 58.0$  MPa (8.41 ksi) for Equation 8 and  $\pm 45.5$  MPa (6.60 ksi) for Equation 9. From Figs. 6 and 7, it can be seen all data points lie within the 95% confidence interval. Thus, the model equation expressed in Equation 5 appears to be effective for predicting the tensile strength of resistance-brazed joints.

## Results and Discussion

### Improvement of Prediction

Although the calculated results using the model equation expressed in Equation 5 show good agreement with the experimental data, further experiments and modeling should be performed to improve prediction methods of the tensile strength of resistance-brazed joints.

The response time of the transducer used in the present work was 0.25 s. Since this response time is not sufficiently short to be compared with the energizing time of 0.8 s, there will be some degree of error in the electric current measure-

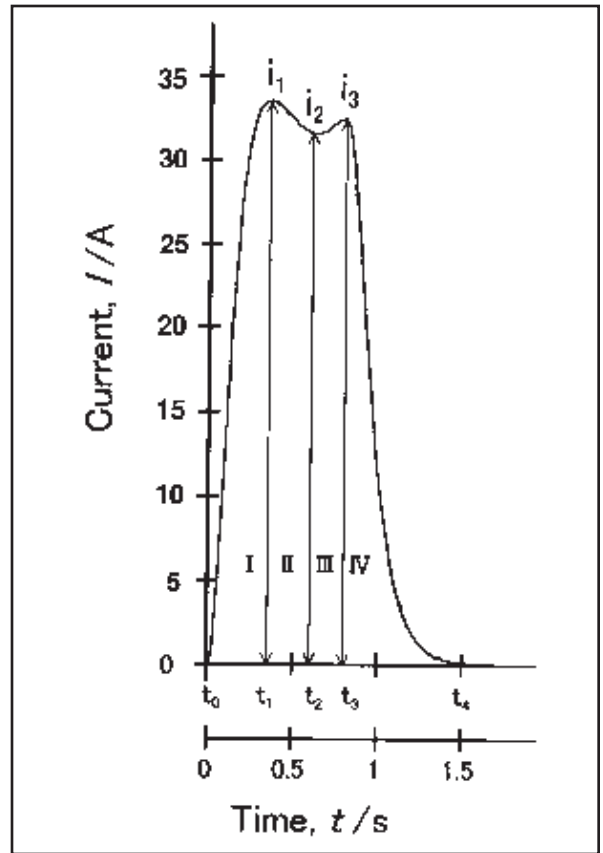


Fig. 5 — Typical electric current curve.

ment. As stated previously, the unknown parameters in the model equation were determined using experimental data, including this error. Therefore, if the degree of error in the experimental data can be reduced using a transducer with a shorter response time, the prediction model equation could be greatly improved.

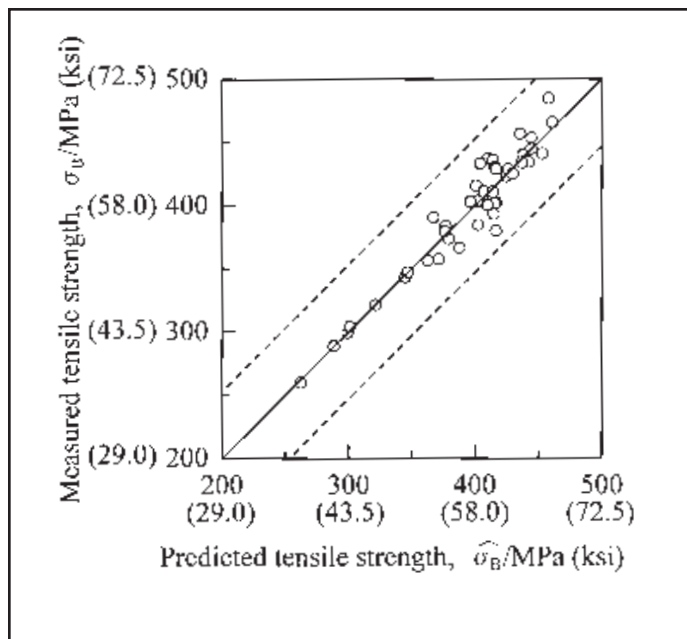


Fig. 6 — Relationship between measured and predicted tensile strength of joints resistance brazed with Ti-Zr-Ni-Cu filler metal. Two dashed lines indicate an approximate 95% confidence interval.

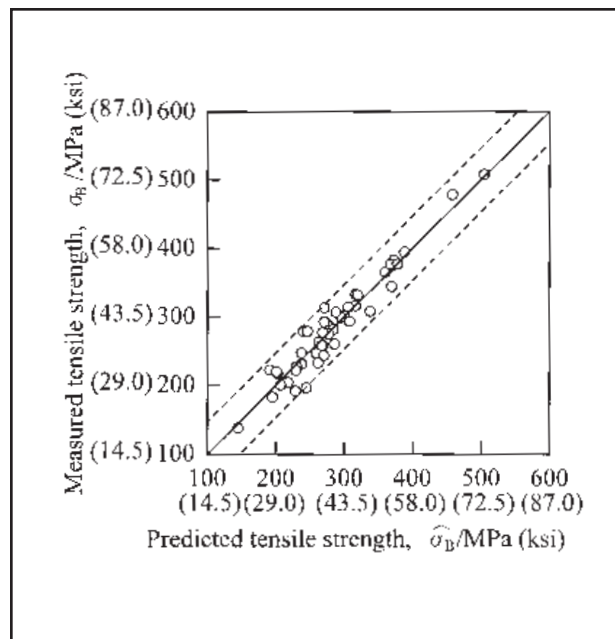


Fig. 7 — Relationship between measured and predicted tensile strength of joints resistance brazed with Ni-Cu filler metal. Two dashed lines indicate an approximate 95% confidence interval.

The model equation expressed in Equation 5 was derived by making some assumptions. To improve the prediction model equation, these assumptions should be confirmed experimentally by examining the compositional change in the solidified filler metal and by measuring the spacing between the base metals. These experimental results may enable a better model equation to be derived with respect to the three extremum values in the electric current during resistance brazing, leading to improved prediction of the tensile strength of resistance-brazed joints.

## Conclusions

The results of the present work provided the following conclusions.

1) During resistance brazing, the electric current passing through the primary circuit of the transformer changes in relation to the three extremum values,  $i_1$ ,  $i_2$  and  $i_3$ . The electric current rapidly increased to the first maximum value,  $i_1$ , then gradually decreased to the minimum value,  $i_2$ , and finally gradually increased to the second maximum value,  $i_3$ .

2) The tensile strength of resistance-brazed joints was predicted using a model equation expressed in the form of a polynomial in three variables of  $i_1$ ,  $i_1-i_2$  and  $i_2/i_3$ . The predicted tensile strength of Ti-10 wt-% Zr alloy joints resistance brazed with Ti-20 wt-% Zr-20

wt-% Ni-20 wt-% Cu or Ni-50 wt-% Cu filler metal agreed well with experimental data. The values of the multiple correlation coefficient adjusted for the degrees of freedom were 0.883 for Ti-20 wt-% Zr-20 wt-% Ni-20 wt-% Cu filler metal and 0.884 for Ni-50 wt-% Cu filler metal.

## Acknowledgment

The author would like to acknowledge the contributions of Ken Tanimukai and Hidekazu Fujimura, who performed the measurements and calculations.

## References

1. Nishimatsu, C., and Gurland, J. 1960. Experimental survey of the deformation of the hard-ductile two-phase alloy system WC-Co. *Transactions of the ASM* 52: 469-484.
2. Doi, H., Fujiwara, Y., and Miyake, K. 1969. Mechanism of plastic deformation and dislocation damping of cemented carbides. *Transactions of the Metallurgical Society of AIME* 245: 1457-1470.
3. Bredzs, N. 1954. Investigation of factors determining the tensile strength of brazed joints. *Welding Journal* 33(11): 545-s to 562-s.
4. O'Brien, M., Rice, C. R., and Olson, D. L. 1976. High strength diffusion welding of silver coated base metals. *Welding Journal* 55(1): 25-27.
5. Takeshita, K., and Terakura, Y. 1998. A novel approach for predicting the tensile strength of brazed joints. *Metallurgical and Materials Transactions A* 29A(2): 587-592.

6. Reed-Hill, R. E. 1973. *Physical Metallurgy Principles*, 2nd. ed. D. Van Nostrand Co., p. 384.

7. Reed-Hill, R. E. 1973. *Physical Metallurgy Principles*, 2nd. ed. D. Van Nostrand Co., p. 412.

8. Draper, N. R., and Smith, H. 1966. *Applied Regression Analysis*. New York, N.Y., John Wiley & Sons, p. 147.

9. Okuno, T., Kume, H., Haga, T., and Yoshizawa, T. 1981. *Multivariate Analysis* (in Japanese). Nikka Giren Pub. Co., p. 152.

10. Okuno, T., Kume, H., Haga, T., and Yoshizawa, T. 1981. *Multivariate Analysis* (in Japanese). Nikka Giren Pub. Co., p. 45.

11. Hoel, P. G. 1971. *Elementary Statistics*, 3rd. ed. New York, N.Y., John Wiley & Sons, p. 204.

## REPRINTS REPRINTS

To Order Custom Reprints  
of Articles in the  
*Welding Journal*

Call Denis Mulligan  
at (800) 259-0470

## REPRINTS REPRINTS